Development 137, 1327-1337 (2010) doi:10.1242/dev.045971

Prostaglandin Gβγ signaling stimulates gastrulation movements by limiting cell adhesion through Snai1a stabilization

Christina K. Speirs[1], Kristin K. Jernigan[2], Seok-Hyung Kim[1], Yong I. Cha[3], Fang Lin[1,4], Diane S. Sepich[1], Raymond N. DuBois[3,5], Ethan Lee[2] and Lilianna Solnica-Krezel[1,6,*]

SUMMARY

Gastrulation movements form the germ layers and shape them into the vertebrate body. Gastrulation entails a variety of cell behaviors, including directed cell migration and cell delamination, which are also involved in other physiological and pathological processes, such as cancer metastasis. Decreased Prostaglandin E_2 (PGE_2) synthesis due to interference with the Cyclooxygenase (Cox) and Prostaglandin E synthase (Ptges) enzymes halts gastrulation and limits cancer cell invasiveness, but how PGE_2 regulates cell motility remains unclear. Here we show that PGE_2-deficient zebrafish embryos, impaired in the epiboly, internalization, convergence and extension gastrulation movements, exhibit markedly increased cell-cell adhesion, which contributes to defective cell movements in the gastrula. Our analyses reveal that PGE_2 promotes cell protrusive activity and limits cell adhesion by modulating E-cadherin transcript and protein, in part through stabilization of the Snai1a (also known as Snail1) transcriptional repressor, an evolutionarily conserved regulator of cell delamination and directed migration. We delineate a pathway whereby PGE_2 potentiates interaction between the receptor-coupled G protein βγ subunits and Gsk3β to inhibit proteasomal degradation of Snai1a. However, overexpression of β-catenin cannot stabilize Snai1a in PGE_2-deficient gastrulae. Thus, the Gsk3β-mediated and β-catenin-independent inhibition of cell adhesion by Prostaglandins provides an additional mechanism for the functional interactions between the PGE_2 and Wnt signaling pathways during development and disease. We propose that ubiquitously expressed PGE_2 synthesizing enzymes, by promoting the stability of Snai1a, enable the precise and rapid regulation of cell adhesion that is required for the dynamic cell behaviors that drive various gastrulation movements.

KEY WORDS: Prostaglandin E_2, Gβγ, Gastrulation, Cell adhesion, Snail, Zebrafish

INTRODUCTION

Prostaglandin signaling is important for homeostasis and contributes to digestion, reproduction, pain, immunity, cardiovascular function and stem cell recovery (Wang and Dubois, 2006). In addition, Prostaglandin E_2 (PGE_2) function is associated with increased cancer cell proliferation, anchorage independence (the ability of a cell to survive without anchorage to an extracellular matrix), invasion and angiogenesis in a variety of tumor types, including colorectal, hepatocellular, transitional bladder carcinoma, medullary thyroid, gall bladder and breast cancer (Buchanan and Dubois, 2006; Wang and Dubois, 2006; Backlund et al., 2008). PGE_2 synthesis begins when arachidonic acid, synthesized from membrane phospholipids, forms PGG_2/PGH_2 through the action of Cyclooxygenases (Cox) 1 and 2 [also known as Prostaglandin-endoperoxide synthases (Ptgs) and Prostaglandin G/H synthases (Pghs)]. PGH_2 is converted by Prostaglandin E synthase (Ptges) to PGE_2, which binds and signals via its downstream G-protein-coupled receptors (GPCRs) E-prostanoid (EP) 1-4 [also known as Prostaglandin E receptors (Ptger)] (see Fig. S1A in the supplementary material) (Regan, 2003; Wu, 2006).

Normal fertility and gestation require prostaglandins. Thus, the phenotypes of mouse mutants with inactive components of prostaglandin synthesis or signaling cannot clarify a role for prostaglandins during embryogenesis (Cha et al., 2006b). However, studies in zebrafish, which develop outside the mother, have shown that prostaglandins are required for early vertebrate embryogenesis, specifically gastrulation, a key process of cell signaling and cell movement that structures the body plan (Grosser et al., 2002; Solnica-Krezel, 2005; Cha et al., 2006a). There are four evolutionarily conserved gastrulation movements: epiboly, internalization, convergence and extension (see Fig. S1B,C in the supplementary material). Epiboly, the initial movement of zebrafish gastrulation, thins and spreads embryonic tissues over the yolk cell. During internalization, mesendodermal progenitors move underneath the prospective ectoderm. Following internalization, mesendodermal cells migrate towards the animal pole, the future head of the embryo. The movements of convergence and extension narrow the germ layers and embryonic body mediolaterally, while extension movements elongate the embryonic tissues head to tail (Solnica-Krezel, 2005). Each of these cell movements is the outcome of individual cell migratory behaviors that, interestingly, require cell signaling pathways, such as Phosphoinositide-3-kinase (Pik3/Pi3K), that are conserved in migrating cancer cells (Montero et al., 2003; Fujino et al., 2002; Fujino and Regan, 2003).

[1]Department of Biological Sciences, Vanderbilt University, Nashville, TN 37232, USA. [2]Department of Cell and Developmental Biology, Vanderbilt University Medical Center, Nashville, TN 37232, USA. [3]Department of Medicine and Cancer Biology, Cell and Developmental Biology, Vanderbilt University Medical Center and Vanderbilt Ingram Cancer Center, Nashville, TN 37232, USA. [4]Department of Anatomy and Cell Biology, Carver College of Medicine, University of Iowa, Iowa City, IA 52242, USA. [5]M. D. Anderson Cancer Center, University of Texas, Houston, TX 77030, USA. [6]Department of Developmental Biology, Washington University School of Medicine, St Louis, MO 63110, USA.

*Author for correspondence (lilianna.solnica-krezel@vanderbilt.edu)

Accepted 15 February 2010

Previously, prostaglandin synthesis in zebrafish embryos was reduced with enzymatic inhibitors of Cox1 (Ptgs1– Zebrafish Information Network) or antisense morpholino oligonucleotides (MO) that inhibit the translation of Cox1 (*cox1* MO, MO1-*ptgs*) or Ptges (*ptges* MO, MO2-*ptges*). These manipulations resulted in an epiboly delay or arrest, largely owing to depletion of PGE_2, the predominant prostaglandin in zebrafish gastrulae (Grosser et al., 2002; Cha et al., 2006a). Additionally, lowering PGE_2 signaling with a low dose of *ptges* MO (2 ng) resulted in a convergence and extension defect due to the decreased speed of dorsally migrating lateral mesodermal cells (Cha et al., 2006a), suggesting that different gastrulation movements require distinct levels of PGE_2.

Here, we extend these analyses to reveal that PGE_2 influences all of the gastrulation movements in zebrafish. We have characterized the movement defects manifest in PGE_2-deficient gastrulae by time-lapse imaging to evaluate cell motility and protrusive activity, and found that both are impaired with decreased PGE_2 synthesis. Further analysis revealed that embryos with decreased PGE_2 have markedly increased cell-cell adhesion, which might contribute to the observed movement defects and is the first evidence that PGE_2 limits cell adhesion during development. We also delineate a signaling mechanism whereby PGE_2 stabilizes the Snai1a protein, an inhibitor of *E-cadherin* (*cdh1*) transcription (Barrallo-Gimeno and Nieto, 2005), by preventing its proteasomal degradation as promoted by Gsk3β. Furthermore, PGE_2 limits the inhibition of Snai1a by Gsk3β by potentiating a novel interaction between the Gβγ effector subunits of PGE_2 signaling and Gsk3β. We propose that ubiquitously expressed PGE_2 synthesizing enzymes promote the stability of Snai1a to allow precise and rapid regulation of the cell adhesion that is required for the dynamic cell behaviors of gastrulation.

MATERIALS AND METHODS

Zebrafish strains and maintenance

Embryos were obtained from natural matings and staged according to morphology as described (Kimmel et al., 1995). With the exception of experiments using the MZ *oep*$^{tz57/tz57}$ (Gritsman et al., 1999) and the Tg(*gsc*:GFP)$^{+/+}$ (Doitsidou et al., 2002), all experiments were performed using wild-type embryos.

Embryo injection

Zebrafish embryos were injected at the one-cell stage, 15-45 minutes post-fertilization. The injected antisense MOs included the control MO/5-bp-mismatch MO2-*ptges* (5′-GTTTTATCCTGTTAGGTC-3′), *ptges* MO/MO2-*ptges* (Cha et al., 2006a), *cox1* MO/MO1-*ptgs* (Grosser et al., 2002) and *cdh1* MO/MO3-*cdh1* (Babb and Marrs, 2004). RNA constructs for synthetic RNA used for injection included *megfp*, *yfp* (Yamashita et al., 2004), *zsnai1a-yfp* (T. Hirano laboratory, Osaka University, Osaka, Japan) (Yamashita et al., 2004), *zgsk3*β (M. Hibi, Riken Center for Developmental Biology, Kobe, Japan), *h*β*1*, *h*γ*2*, *ΔN*β*-catenin* and *ndr2*/*cyclops* (C. V. Wright laboratory, Vanderbilt University, Nashville, TN, USA) (Erter et al., 1998). Embryos were injected with *snai1a-HA* RNA at the 8- to 16-cell stage. All RNA constructs were in the pCS2 vector.

Snai1a-YFP assay

Injected embryos were chemically treated as described below and incubated at 28°C until the shield stage. All experiments described were performed at least three times with at least 30 injected embryos per sample (per experiment). Live embryos were oriented using the shield as a morphological landmark in 2% Methylcellulose/0.3× Danieau. Representative embryos were imaged on an LSM 510 confocal microscope (Carl Zeiss MicroImaging, Thornwood, NY, USA), using the 10× objective. Experiments were performed in part through the VUMC Cell Imaging Shared Resource. Images were prepared for publication using Volocity software (Improvision, Coventry, UK) and Adobe Photoshop (Adobe, San Jose, CA, USA).

Embryo treatment

PGE_2

Embryos were treated in 1% DMSO/embryo medium with synthetic PGE_2 (10 mM; Cayman Chemical, Ann Arbor, MI, USA) at two time points: following injection and at the dome stage (Cha et al., 2006a).

Proteasomal inhibitor

Embryos were treated with Z-Leu-Leu-Leu-H/MG-132 (Peptide Institute, Minoh, Osaka, Japan) (50 mM) (Zhou et al., 2004) from the 128- to 256-cell stage in 1% DMSO/embryo medium until the embryos were imaged at the shield stage.

Gsk3β inhibitor

LiCl treatment was performed as described (Stachel et al., 1993). LiCl (Sigma-Aldrich, St Louis, MO, USA) (0.3 M) was added to the embryo medium at the 256-cell stage for 10 minutes, the embryos then rinsed three times in 0.3× Danieau and incubated until the shield stage. Gsk3β BIO (Stemgent, Cambridge, MA, USA) (1 μM) was added at the 1000-cell stage and left until the shield stage.

Pik3 inhibitor

Embryos were incubated in 30-50 μM LY294002 (Caymen Chemical) in embryo medium from the dome until the shield stage.

Cell adhesion assays

Cell adhesion assays were performed essentially as described (Ulrich et al., 2005). The cells from dissociated blastulae were diluted to 50,000 cells/ml and plated in a fibronectin-coated 96-well plate (5000 cells/well). Images were taken on a SteREO Discovery V12 Dissecting Microscope (Carl Zeiss MicroImaging) every hour for 3 hours.

Quantitative real-time (qRT) PCR

RNA was extracted from 20 injected embryos per sample at 60% epiboly using 200 μl Trizol (Tingaud-Sequeira et al., 2004). Following RNA extraction, the samples were diluted to 50 ng/μl. Primers included β-*actin* (Tingaud-Sequeira et al., 2004), *cdh1* (forward, 5′-TGAAGGCTGCA-GATAACGAC-3′; reverse, 5′-GTGTTGAGGGAGCTGAGTGA-3′) and *snai1a* (forward, 5′-GAGCTGGAATGTCAGAACGA-3′; reverse, 5′-GT-GAAGGGAAGGTAGCAAGC-3′). Samples were prepared for qRT-PCR using the iScript One-Step RT-PCR Kit with SYBR Green (Bio-Rad, Hercules, CA, USA). For each sample, 100 ng of template DNA was used, and water was used as a negative control for the no reverse transcriptase (–RT) reaction. The qRT-PCR was performed on an iCycler iQ Multicolor machine (Bio-Rad) at the VUMC Molecular Biology Resource Core. The annealing temperature was 60°C without a temperature gradient. The data shown represent three separate experiments with duplicate samples. The data were analyzed with iQ5 Optical System Software, version 2.0 (Bio-Rad).

Time-lapse imaging

Shield time-lapse

Embryos were injected with *membrane egfp* RNA. At the shield stage, embryos were dechorionated in 0.3× Danieau and oriented in Matek PG35G-0-10-C glass-bottom dishes using 0.8% SeaPlaque Low-Melt Agarose (Lonza, Rockland, ME, USA) in 0.3× Danieau. Images were taken of the shield on a Zeiss Axiovert 200 inverted microscope (Carl Zeiss MicroImaging) with an ERS Spinning Disk Confocal system (PerkinElmer, Fremont, CA, USA) using the 40× oil-immersion (N.A.=1.3) objective. Images of *z*-sections (0.5 μm) were taken every minute. The resulting data points were orthogonally reconstructed using Volocity software.

Protrusion movie analysis

membrane egfp or *membrane rfp* RNA was injected into Tg(*gsc*:GFP)$^{+/+}$ zebrafish embryos (labeled donor embryos). Fewer than ten cells were transplanted from donor embryos to unlabeled host embryos at the shield stage. Host embryos containing transplanted cells that were *gsc*:GFP-positive were mounted at 70-80% epiboly in SeaPlaque agarose in 0.3× Danieau in glass-bottom dishes as described above, with the shield facing downward. Images were taken on the Axiovert 200 inverted microscope/ERS Spinning Disk Confocal system using the 40× oil-immersion

(N.A.=1.3) objective for 5-10 minutes, with two to three *z*-planes taken every 10 seconds (*z*-planes of 2.8-5 μm). All time-lapse movies were processed using Volocity, Adobe Photoshop and QuickTime Pro software.

Whole-mount in situ hybridization (ISH)

Embryos were collected at the indicated stage and fixed with 4% paraformaldehyde overnight at 4°C. Whole-mount ISH was performed as described (Thisse and Thisse, 1998). Probes included *snai1a* (Hammerschmidt and Nusslein-Volhard, 1993), *snai1b* (Blanco et al., 2007), *frizzled 8b* (Kim et al., 1998) and *no tail* (Schulte-Merker et al., 1992).

Western blot

Embryos were homogenized with RIPA buffer (10 mM Tris-HCl pH 7.4, 150 mM NaCl, 1 mM EDTA, 0.1% SDS, 1% Triton X-100, 1% sodium deoxycholate), then frozen at –20°C. Embryo homogenates were lysed with 2× lysis buffer (62.5 mM Tris-HCl pH 6.8, 10% glycerol, 2% SDS, 0.5% β-mercaptoethanol, 0.01% Bromophenol Blue) and heated at 100°C for 5 minutes. Extracts were resolved in a 4-15% polyacrylamide gel and transferred to a PVDF membrane using the Criterion System (Bio-Rad). The antibodies used were anti-zebrafish Snai1 (1:500; Hammerschmidt laboratory, Max-Planck-Institute of Immunobiology, Freiburg, Germany) (Hammerschmidt and Nusslein-Volhard, 1993), anti-zebrafish E-cadherin (1:1000; J. A. Marrs laboratory, Indiana University Medical Center, Indianapolis, IN, USA) (Babb and Marrs, 2004), anti-Gsk3β (1:1000; Cell Signaling Technology, Danvers, MA, USA), anti-phospho-Gsk3β (1:1000; Cell Signaling Technology) and anti-Gapdh (1:500; RDI Division of Fitzgerald Industries, Concord, MA, USA). For full scans of all western blots depicted, see Fig. S5 in the supplementary material.

Whole-mount immunohistochemistry

Zebrafish embryos were collected at the indicated stage and fixed with a 1:1 solution of 8% paraformaldehyde and 2× fix buffer (8% sucrose, 0.3 mM $CaCl_2$ in PBS pH 7.3). Embryos were rinsed four times with PBS containing 0.1% Tween 20. Antibodies used were anti-zebrafish E-cadherin (as above) and anti-ZO1 (Tjp1) (1:200; Zymed Laboratories, San Francisco, CA, USA). To visualize nuclei, samples were stained with SYTO 59 (Invitrogen) for 30 minutes prior to imaging, then rinsed twice with PBS containing 0.1% Tween 20 and 2% DMSO.

Cell culture, transfection and immunoprecipitation

HEK-293T cells were cultured in DMEM (Cellgro) media supplemented with 100 units/ml penicillin, 100 unit/ml streptomycin (Gibco) and 10% fetal bovine serum (FBS) (Gibco). Lipofectamine 2000 (Invitrogen) was used for transfections following the manufacturer's protocol. HEK-293T cells were plated in 30 mm plates and transfected with 1 μg Gsk3β, 1 μg HA-Gβ1, 1 μg Gγ$_2$ and 2 μg c-βark (all vectors are pCS2), and cultured for 48 hours post-transfection. For the PGE$_2$ treatment, cells were then treated with 0.1, 1 and 10 μM PGE$_2$ for 14 hours. Cells were washed once with cold PBS and then lysed for 30 minutes on ice in non-denaturing lysis buffer (NDLB) comprising 50 mM Tris-HCl pH 7.4, 300 mM NaCl, 5 mM EDTA, 1% (w/v) Triton X-100 and protease inhibitors (1 mg/ml leupeptin, pepstatin and chymostatin). Then, 750 μg of lysate was diluted to 1 mg/ml with NDLB. Rat anti-HA (Roche) was cross-linked to protein G magnetic beads (New England Biologicals) following the manufacturer's protocol. Anti-HA protein G beads were then added to the lysate and incubated for 2 hours with rotation at 4°C. Beads were then washed three times with NDLB and once or twice with PBS. Protein was eluted from the beads with sample buffer. Samples, as well as 10 μg of total protein lysate, were then run on SDS-PAGE gels and transferred to a nitrocellulose membrane. Membranes were blocked in 5% milk solution (1 hour at room temperature) and probed with mouse anti-HA (1:1000; 12CA5, Santa Cruz, CA, USA), mouse anti-α-tubulin (1:3000; DM1a, Sigma) and mouse anti-Gsk3 (1:1000; BD Biosciences) for the immunoprecipitation without PGE$_2$ treatment, and with rabbit anti-Gβ (1:500; T-20, Santa Cruz), mouse anti-α-tubulin (as above), and rabbit anti-Gsk3 (1:1000; 27C10, Cell Signaling) for the immunoprecipitation after PGE$_2$ treatment. HRP-conjugated anti-mouse and anti-rabbit antibodies were used to detect primary antibody by chemiluminescence.

Statistical analysis

Statistical analyses of the qRT-PCR and cell behavior experiments were performed with Microsoft Excel software. The raw data were processed to calculate the mean and the s.e.m. (as indicated by error bars in the figures). Statistical significance was evaluated by Student's *t*-test.

RESULTS

Decreased PGE$_2$ synthesis results in global cell movement defects during gastrulation

To detail the mechanisms by which PGE$_2$ regulates gastrulation, we focused on higher dose (4 ng) MO2-*ptges*-injected embryos that displayed strong and global gastrulation defects (Fig. 1A-C), paralleling those reported for *cox1* MO or enzymatic inhibitors (Grosser et al., 2002; Cha et al., 2006a). These defects in *ptges* morphants were suppressed by supplementing the embryo medium with PGE$_2$ and were not observed when a control 5-bp-mismatch MO (control MO) was injected. Ptges- and Cox1-deficient gastrulae showed arrested epiboly and an uneven surface associated with cell clumping (Fig. 1A; see Fig. S2A in the supplementary material). Whereas chordamesodermal cells expressing *no tail* (*ntl*; also known as *brachyury*) were in the deeper, mesendodermal layer of control morphant gastrulae, Ptges-deficient gastrulae had *ntl*-expressing cells in the superficial layer, indicating that internalization was defective in the most strongly affected embryos (Fig. 1B). In less severely affected Ptges-deficient gastrulae, internalization did occur (Fig. 1C). However, migration towards the animal pole, representing the subsequent movement of mesodermal cells, was impaired relative to that in control gastrulae, as indicated by the posteriorly shifted position of *frizzled homolog 8b* (*fzd8b*)-expressing prechordal mesoderm cells (Fig. 1C). All these movement defects were partially suppressed with synthetic PGE$_2$ treatment, confirming the specific and essential role of PGE$_2$ in gastrulation movements. Defective gastrulation movements, cell paths and net speed were also revealed by time-lapse analysis of the dorsal shield, which is equivalent to the Spemann-Mangold organizer of amphibians (Fig. 1D,E; see Fig. S1F and Movies 1, 2 in the supplementary material). In addition, the boundary (Brachet's cleft) between the internalized mesendodermal cells and the superficial layer was distinct in the control, but unclear in Ptges-deficient, gastrulae (Fig. 1D; see Movies 1, 2 in the supplementary material). Together, these data reveal that PGE$_2$ signaling is essential for epiboly and internalization in addition to convergence and extension movements during gastrulation (Grosser et al., 2002; Cha et al., 2006a).

PGE$_2$ synthesis is required for normal protrusion formation in gastrula cells

Defects in cell movements during gastrulation can occur as a result of impaired protrusive activity, cell adhesion, cytoskeleton dynamics and cell polarity (Montero et al., 2003; Montero and Heisenberg, 2004; Solnica-Krezel, 2005; Ulrich et al., 2005). Thus, we sought to evaluate how cell motility was undermined in Ptges-deficient embryos. First, we analyzed protrusive activity, which, when defective, can hinder the motility of gastrula cells (Montero et al., 2003). Time-lapse imaging of membrane EGFP-labeled cells demonstrated that at the interface of the blastoderm and the yolk cell during early gastrulation, cells exhibited protrusions with few blebs in the control morphants (see Fig. S1D in the supplementary material). *ptges* morphant cells, however, showed increased blebbing (see Fig. S1E in the supplementary material). From 60-90% epiboly, the protrusions of the prechordal mesodermal cells migrating towards the animal pole in control gastrulae were active and dynamic, with filopodial characteristics (Montero et al., 2003),

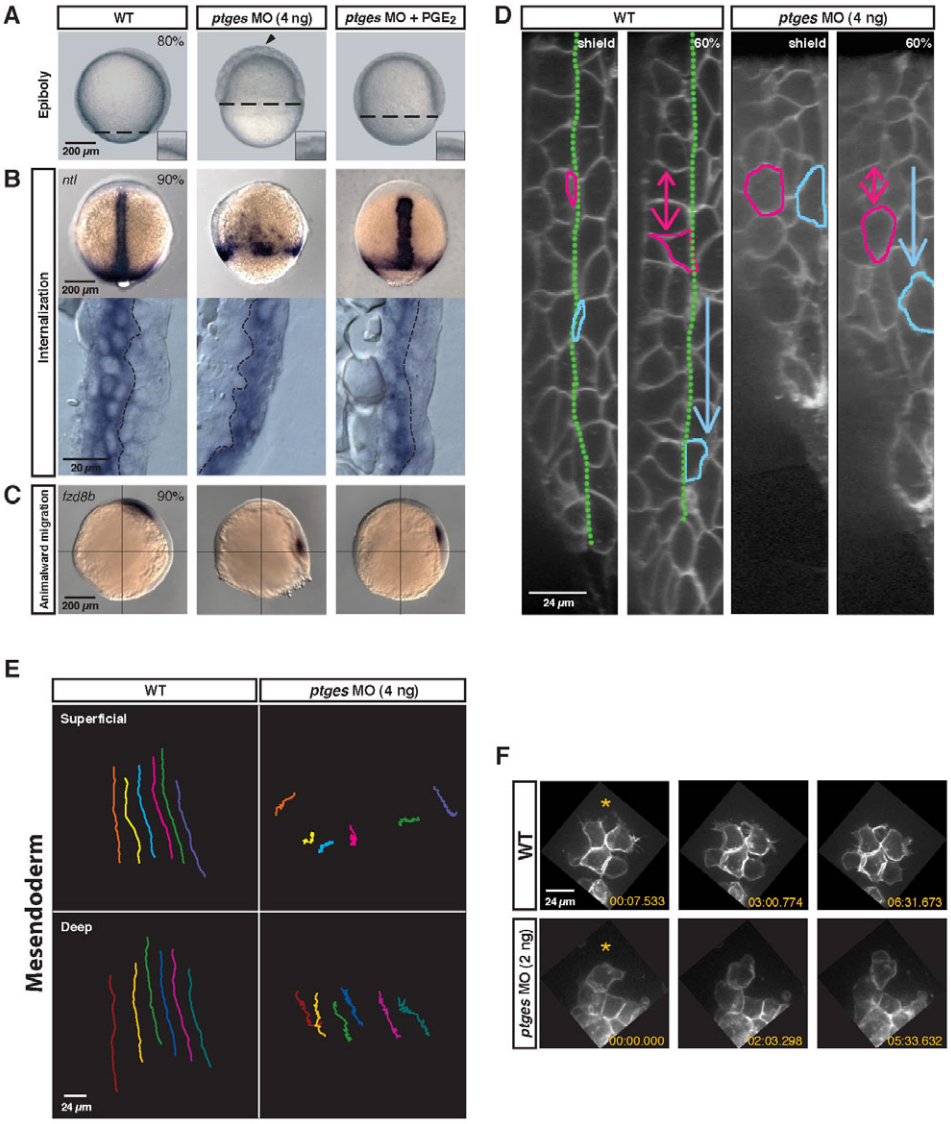

Fig. 1. Depletion of PGE_2 causes global gastrulation defects. *ptges* MO-injected (4 ng) zebrafish embryos were evaluated for gastrulation movement defects. (**A**) Live embryos (80% epiboly). WT, uninjected wild type; *ptges* MO (4 ng), Ptges-deficient; *ptges* MO (4 ng) + PGE_2, Ptges-deficient embryos treated with 10 mM PGE_2. Dashed line indicates the progress of epiboly. Arrowhead indicates the uneven surface of the blastoderm. The inset shows the blastoderm surface at high magnification. (**B**) (Top) Deficit of internalized *no tail*-expressing axial mesodermal cells in *ptges* morphants (90% epiboly; dorsal views). (Bottom) Lateral views of cryosections through the dorsal side of the embryo. Yolk cell, left; external surface, right; dashed line, germ layer boundary. (**C**) Migration of *fzd8b*-expressing prechordal mesoderm cells towards the animal pole (90% epiboly; lateral views). (**D**) Confocal images (lateral view) of the dorsal midline in membrane EGFP-labeled embryos at shield stage. Yolk cell, left; external surface, right. The green line marks the boundary between the superficial (blue cell) and deep layers (pink cell) of the gastrula. Arrows indicate the vector of movement. (**E**) The paths of six cells in the superficial and deep layers of the mesendoderm in wild-type and *ptges* morphant embryos. Vegetal pole, top; animal pole, bottom. (**F**) Confocal images of prechordal mesoderm cells (70% epiboly). Three frames from a time-lapse movie are shown. Orange asterisks are towards the animal pole.

and all protrusions localized to the leading edge of the cell (Fig. 1F; see Fig. S1G-I and Movie 3 in the supplementary material). By contrast, the protrusions of the prechordal mesodermal cells in gastrulae with reduced Ptges function (2 ng MO) were blunted, with lamellipodial, sometimes bleb-like, characteristics (Montero et al., 2003). Moreover, protrusions localized to all cell edges (Fig. 1F; see Fig. S1H and Movie 4 in the supplementary material). Therefore, impaired gastrulation movements in PGE_2-depleted embryos are associated with abnormal protrusive activity.

PGE_2 negatively regulates cell-cell adhesion in zebrafish gastrulae

Unbalanced cell adhesion, either in excess or deficit, cripples the movement of primordial germ cells in zebrafish, of border cells in *D. melanogaster* and gastrulation movements in many animals (Blaser et al., 2005; Pacquelet and Rorth, 2005; Hammerschmidt and Wedlich, 2008). In particular, normal gastrulation in all animals requires appropriate levels of E-cadherin (also known as Cadherin 1 or epithelial Cdh1) (Solnica-Krezel, 2006; Hammerschmidt and Wedlich, 2008), a component of the adherens junction that binds β-catenin (Drees et al., 2005). Moreover, zebrafish *cdh1* [also known as *half baked* (*hab*)] mutants manifest defects in epiboly, internalization, convergence and extension (Babb and Marrs, 2004; Kane et al., 2005; McFarland et al., 2005; Montero et al., 2005; Shimizu et al., 2005; von der Hardt et al., 2007). The requirement of direct and indirect inhibitors of E-cadherin, namely $G\alpha_{12/13}$, Wnt11 and p38 (Mapk14a), for normal gastrulation movements underscores the significance of the precise and diverse regulation of cell adhesion in this process (Lin et al., 2005; Ulrich et al., 2005; Zohn et al., 2006; Lin et al., 2009).

Because of the cell clumping observed in Ptges-deficient gastrulae (Fig. 1A), we hypothesized that increased cell adhesion contributed to the gastrulation movement phenotype. To evaluate cell adhesion in Ptges-deficient embryos, we carried out cell adhesion assays using zebrafish embryonic cells ex vivo (Ulrich et al., 2005). First, we induced mesendodermal fates in embryonic cells by co-injecting zygotes with synthetic *nodal-related 2* (*ndr2*; also known as *cyclops* and *znr1*) RNA (see Fig. S2F in the supplementary material) and *ptges* or control MOs. The resulting embryos were dissociated into single cells at the dome stage, then seeded into fibronectin-coated wells for a 3-hour time-course to determine whether cells had formed aggregates. Cells from control morphants showed clumps of two or three cells at the end

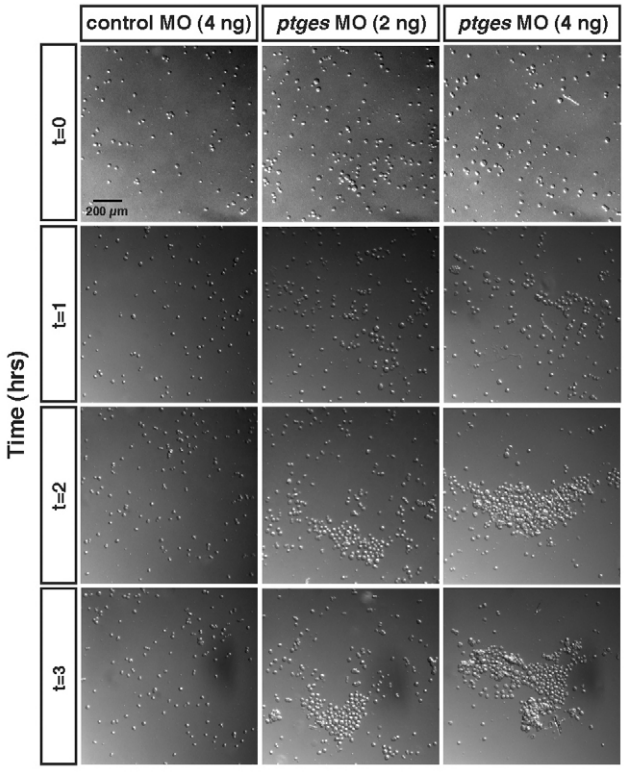

Fig. 2. Decreased PGE$_2$ results in dramatically enhanced embryonic cell-cell adhesion. Cell adhesion assay of cells from dissociated control and *ptges* morphant gastrulae. Images of dissociated blastomeres on the fibronectin substrate were taken every hour for 3 hours. Note the clumping of cells in the Ptges-deficient gastrulae.

of the 3-hour time-course. Strikingly, the *ptges* MO injection increased cell clumping in a dose-dependent manner. In fact, at the end of the experimental period, most of the cells from embryos injected with the high MO dose were in one or two large three-dimensional clumps (containing thousands of cells) that dominated the well (Fig. 2). We conclude that cell adhesion is increased in Ptges-deficient gastrulae, indicating that PGE$_2$ signaling can regulate gastrulation movements by limiting cell adhesion.

The excessive cell adhesion in Ptges-deficient gastrulae might be caused by increased E-cadherin. Accordingly, using qRT-PCR we found that *cdh1* transcript levels relative to those of β-*actin* were twofold higher in Ptges-deficient embryos than controls (Fig. 3A). Immunoblotting analysis showed that the protein levels of E-cadherin were increased twofold relative to those in controls (Fig. 3B). Moreover, whole-mount immunohistochemistry revealed that E-cadherin expression was uniformly increased in the mesendoderm of *ptges* morphants (Fig. 3C). Thus, PGE$_2$ functions during gastrulation to limit E-cadherin transcript and protein expression.

To investigate whether disrupting E-cadherin translation could suppress aspects of the gastrulation phenotype in PGE$_2$-deficient gastrulae, we co-injected *cdh1* (MO3-*cdh1*) and *ptges* MOs. Downregulation of E-cadherin suppressed the cell clumping phenotype, but did not significantly improve the epiboly defect (Fig. 3D,E). Hence, enhanced cell adhesion contributes in part to the gastrulation defects seen in Ptges-deficient embryos.

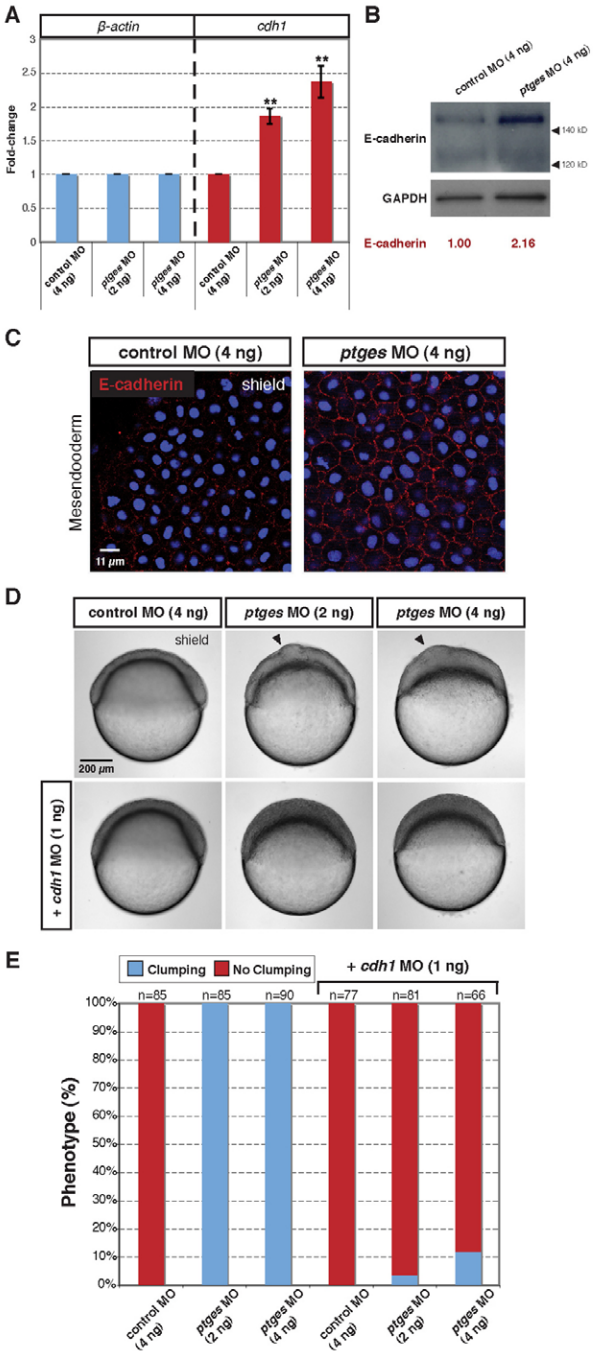

Fig. 3. PGE$_2$ governs cell adhesion by decreasing Cdh1 transcript and protein levels. (**A**) Quantitative real-time PCR (qRT-PCR) of β-*actin* (left) and *cdh1* (right) transcript levels in control and *ptges* morphants at 60% epiboly. **, $P<0.005$. (**B**) Western blot of E-cadherin (top) and Gapdh (bottom, loading control) from shield-stage zebrafish embryos injected with control and *ptges* MOs. The two isoforms of E-cadherin present during zebrafish development have been described previously (Babb and Marrs, 2004); the larger isoform is dominant during gastrulation. (**C**) Confocal images of whole-mount E-cadherin immunostaining. E-cadherin protein expression (red) at the shield stage in the mesoderm (lateral view). Blue, nuclear stain. (**D**) Suppression of the cell clumping phenotype (arrowhead) in *ptges* morphants by *cdh1* MO injection. Embryos are at the shield stage. (**E**) A compilation of two experiments in which control and *ptges* morphant embryos were co-injected with *cdh1* MO (1 ng) and evaluated at 60% epiboly for the cell clumping phenotype.

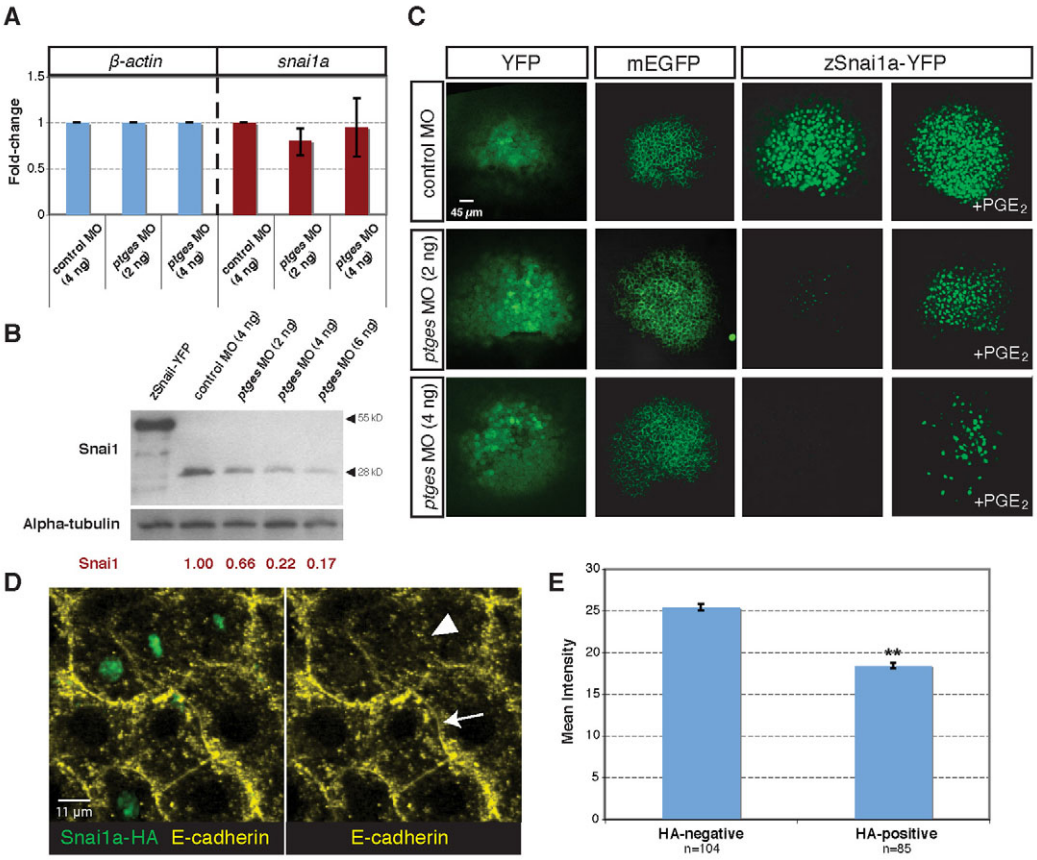

Fig. 4. PGE_2 deficiency destabilizes Snai1a protein. (**A**) qRT-PCR of β-*actin* (left) and *snai1a* (right) transcript levels in control and *ptges* morphants at 60% epiboly. (**B**) Immunoblotting using antibodies against Snai1a (top) and α-tubulin (loading control, bottom) in control and *ptges* morphants. The first lane shows zebrafish embryos that were injected with *snai1a-yfp* (which encodes a protein of 55 kDa). (**C**) Confocal images of Snai1a-YFP, YFP, and membrane EGFP expression in control (top row) and *ptges* morphants (middle and bottom rows), and *ptges* morphants incubated with PGE_2 (shield stage). (**D**) Confocal images of *ptges* morphant gastrulae (shield stage) stained with anti-HA (green) and anti-E-cadherin (yellow) that were mosaically injected with *snai1a-HA* RNA (3 pg) at the 8- to 16-cell stage. Compare the intensity of E-cadherin staining at the membranes between two HA-positive cells (arrowhead) with that between two HA-negative cells (arrow). (**E**) Quantitation of E-cadherin immunostaining intensity (mean intensity) of Snai1a-HA-negative and Snai1a-HA-positive cells in *ptges* morphant gastrulae. **, $P=1.16\times10^{-10}$.

Snai1a protein expression is stabilized in the presence of PGE_2

The increase of *cdh1* transcripts in the Ptges-deficient embryos suggested that PGE_2 signaling positively regulates a transcriptional repressor of the *cdh1* gene. Snai1, the best characterized of these, binds E-boxes in the *E-cadherin* (*cdh1*) promoter to inhibit its transcription (Barrallo-Gimeno and Nieto, 2005). *Snai1* conditional mouse mutants show defective formation of the mesoderm layer because of persistent epithelial morphology, as well as impaired anterior migration of mesodermal cells (Carver et al., 2001). Furthermore, Snai1 is required for internalization movements in *Drosophila* and sea urchin (Barrallo-Gimeno and Nieto, 2005; Wu and McClay, 2007). There are four zebrafish Snail genes, two of which have arisen through duplication of *snai1* in the teleost lineage. *snai1a* and *snai1b* are expressed in the internalizing mesendoderm during gastrulation and are required for the migration of anterior mesendodermal cells towards the animal pole (Hammerschmidt and Nusslein-Volhard, 1993; Yamashita et al., 2004; Blanco et al., 2007). In addition, *snai1b* morphants display convergence and extension defects (Blanco et al., 2007). Altogether, these data imply that Snai1a and Snai1b are required for the gastrulation movements.

Recent work in cell culture has shown that chemical or antisense interference with the prostaglandin signaling pathway components results in decreased *Snai1* transcription and increased E-cadherin protein levels (Dohadwala et al., 2006; Brouxhon et al., 2007). However, our qRT-PCR and whole-mount ISH analyses showed that *snai1a* and *snai1b* levels were not significantly different in *ptges* versus control morphants (Fig. 4A; see Fig. S3A,B in the supplementary material) until 60% epiboly, when the Ptges-deficient gastrulation phenotype is already apparent (see Fig. S3B in the supplementary material). Therefore, we conclude that the regulation of *snai1a* or *snai1b* transcription by PGE_2 could not cause the gastrulation defects in this developmental context. By contrast, western blotting with an anti-Snai1a antibody, raised against the full-length protein (Hammerschmidt and Nusslein-Volhard, 1993), revealed that the Snai1a protein level was significantly reduced in embryos injected with *ptges* MO in a dose-dependent manner (Fig. 4B), demonstrating the post-transcriptional regulation of Snai1a by prostaglandins.

To determine whether the localization or stability of Snai1a was affected in Ptges-deficient gastrulae, we analyzed the expression of the Snai1a-YFP fusion protein (Yamashita et al., 2004) in live embryos. We injected synthetic *snai1a-yfp* (Yamashita et al., 2004),

membrane egfp and *yfp* RNAs containing identical 5′ and 3′ UTR regions into one-cell stage zebrafish embryos and analyzed the resulting proteins by confocal microscopy in the shield stage gastrulae. The injection of *ptges* MO resulted in the dramatic and dose-dependent reduction of Snai1a-YFP expression as compared with that in control embryos (Fig. 4C). By contrast, YFP and membrane (m) EGFP expression were comparable between gastrulae injected with *ptges* and control MOs. Loss of Snai1a-YFP expression in Ptges-deficient gastrulae was suppressed by PGE_2 treatment. Furthermore, *cox1* morphants also showed decreased Snai1a-YFP expression (see Fig. S4B in the supplementary material). Interestingly, injection of RNA encoding Snai1b-YFP showed only a mild decrease in YFP expression in the Ptges-deficient as compared with control gastrulae (see Fig. S3C in the supplementary material). These results demonstrate that PGE_2 signaling can regulate the protein expression of Snai1a and Snai1b. However, Snai1a seems more sensitive to changes in PGE_2 levels than Snai1b.

To test whether the increased *cdh1* transcript and E-cadherin protein levels were an outcome of reduced Snai1a expression, *snai1a-HA* RNA was injected mosaically at the eight-cell stage into embryos injected with *ptges* MO at the one-cell stage (Fig. 4D). The quantification of E-cadherin immunostaining showed that Snai1a-HA-expressing cells had significantly lower E-cadherin levels than surrounding HA-negative cells in these Ptges-deficient gastrulae (Fig. 4E). This suggested that the increased E-cadherin expression in Ptges-deficient mesendodermal cells was suppressed by restored Snai1a expression. Therefore, we conclude that PGE_2 signaling stabilizes Snai1a protein to limit E-cadherin expression during gastrulation.

PGE_2 signaling-associated Gβγ subunits stabilize Snai1a by interaction with Gsk3β

To define the molecular mechanism by which PGE_2 promotes Snai1a stability, we evaluated the outcome of manipulating possible targets of PGE_2 signaling on misexpressed Snai1a-YFP protein levels. First, we tested whether proteolysis contributed to the loss of Snai1a-YFP expression in Ptges-deficient embryos (Dominguez et al., 2003; Zhou et al., 2004). Accordingly, the treatment of Ptges-deficient embryos with a proteasomal inhibitor, MG132 (Zhou et al., 2004), fully suppressed the loss of Snai1a-YFP expression, indicating that proteasomal degradation could decrease Snai1a protein levels (Fig. 5A). Cell culture studies have shown that PGE_2 can regulate Glycogen synthase kinase 3β (Gsk3β) (Fujino et al., 2002; Fujino and Regan, 2003). Given that Gsk3β phosphorylates Snai1, thereby targeting it for proteasomal degradation (Zhou et al., 2004; Yook et al., 2006), we investigated whether this kinase regulates Snai1a expression downstream of PGE_2 signaling. Consistent with this notion, the injection of *gsk3*β RNA significantly decreased the level of misexpressed Snai1a-YFP in a dose-dependent manner in control embryos, and caused the complete loss of Snai1a-YFP in Ptges-deficient gastrulae (Fig. 5B). Conversely, Gsk3β inhibition through either LiCl (Stachel et al., 1993) or 6-bromoindirubin-3-oxime (BIO) (Goessling et al., 2009) treatment, suppressed the reduction of Snai1a-YFP levels in Ptges-deficient gastrulae. Blocking the function of both Gsk3β and the proteasome resulted in the full restoration of Snai1a-YFP levels in Ptges-deficient embryos, similar to embryos treated with proteasomal inhibitor alone (Fig. 5D). Thus, PGE_2 signaling functions to stabilize Snai1a by inhibiting its proteasomal degradation, which is promoted by Gsk3β.

Previous studies indicate that PGE_2 signaling acts in part through heterotrimeric Guanine nucleotide-binding proteins (G proteins) (Buchanan and Dubois, 2006). Following activation of the EP receptors, G protein α and βγ subunits stimulate distinct downstream effectors. Gβγ protein subunits have been shown in cell culture to regulate Gsk3β downstream of PGE_2 signaling by the activation of Pik3 (Fujino et al., 2002; Fujino and Regan, 2003; Cha et al., 2006a). We found that overexpression of the $G\beta_1\gamma_2$ (Gnb1, Gng2) subunits elevated the Snai1a-YFP levels in Ptges-deficient gastrulae, suggesting that the Gβγ subunits activated by the EP receptors were responsible for conveying the effects of PGE_2 on Snai1a (Fig. 5C). Co-injection of RNAs encoding $G\beta_1\gamma_2$ and Gsk3β into Ptges-deficient embryos, however, blocked the rescue of Snai1a-YFP seen with the RNA encoding $G\beta_1\gamma_2$ alone, suggesting that Gsk3β regulates Snai1a downstream of the Gβγ subunits to inhibit Snai1a proteasomal degradation (Fig. 5E; Fig. 6). Accordingly, Gsk3β was detected following the immunoprecipitation of anti-HA in HEK-293T cells co-transfected with zebrafish Gsk3β and HA-human $G\beta_1\gamma_2$. This interaction was inhibited by co-expressing the C-terminal domain of the β-adrenergic receptor kinase (c-βark), which competes for $G\beta_1\gamma_2$ binding (Fig. 5F). These results identify Gsk3β as a potential new Gβγ effector protein downstream of PGE_2 (Fig. 5F). In addition, PGE_2 treatment of transfected HEK-293T cells increased, in a dose-dependent manner, the level of Gsk3β following immunoprecipitation of anti-HA (Fig. 5G), suggesting that PGE_2 can promote the interaction of Gsk3β with Gβγ. This interaction between the Gβγ subunits and Gsk3β provides a novel mechanism for the regulation of the Snai1a protein downstream of PGE_2 signaling.

Next, to determine whether the decreased regulation of Gsk3β by Pik3 contributed to the loss of Snai1a, we overexpressed zebrafish Pik3γ, the form that acts downstream of Gβγ signaling (Leopoldt et al., 1998). We also employed a Pik3 inhibitor, LY294002, which has been shown to impair zebrafish gastrulation (Montero et al., 2003), to investigate the effects of Pik3 downregulation on Snai1a-YFP levels. Overexpression of Pik3γ or inhibition of Pik3 resulted in gastrulation defects as previously observed (Montero et al., 2003) (F.L. and L.S.-K., unpublished observations), confirming that Pik3 activity was being effectively manipulated (data not shown). However, neither treatment significantly altered Snai1a-YFP expression in control or Ptges-deficient embryos (see Fig. S4A in the supplementary material). Thus, the interaction between Gβγ and Gsk3β to regulate Snai1a is unlikely to involve the regulation of Gsk3β by Pik3.

β-catenin does not promote Snai1 stability

The regulation of Gsk3β by Gβγ signaling downstream of PGE_2 presents a possible junction between prostaglandin and Wnt signaling, lending insight into the finding that Cox inhibitors (NSAIDs) decrease the intestinal tumor load of Apc^{min} mouse mutants with unmitigated β-catenin signaling (Buchanan and Dubois, 2006). Wnt8, which activates β-catenin, is expressed in the nascent mesendoderm during gastrulation, similarly to Snai1a (Hammerschmidt and Nusslein-Volhard, 1993; Kelly et al., 1995b; Zohn et al., 2006). Therefore, these two pathways could cooperate to repress cell adhesion by regulating Snai1a through the inhibition of Gsk3β function. Previous data have shown that in cell culture, PGE_2 can bind Axin through its EP2-associated G protein α_s, displacing GSK3β and preventing it from inhibiting β-catenin by proteasomal degradation (Castellone et al., 2005). Moreover, recent work indicates that the Prostaglandin and Wnt pathways converge on Gsk3β through a cAMP/Protein kinase A-dependent mechanism

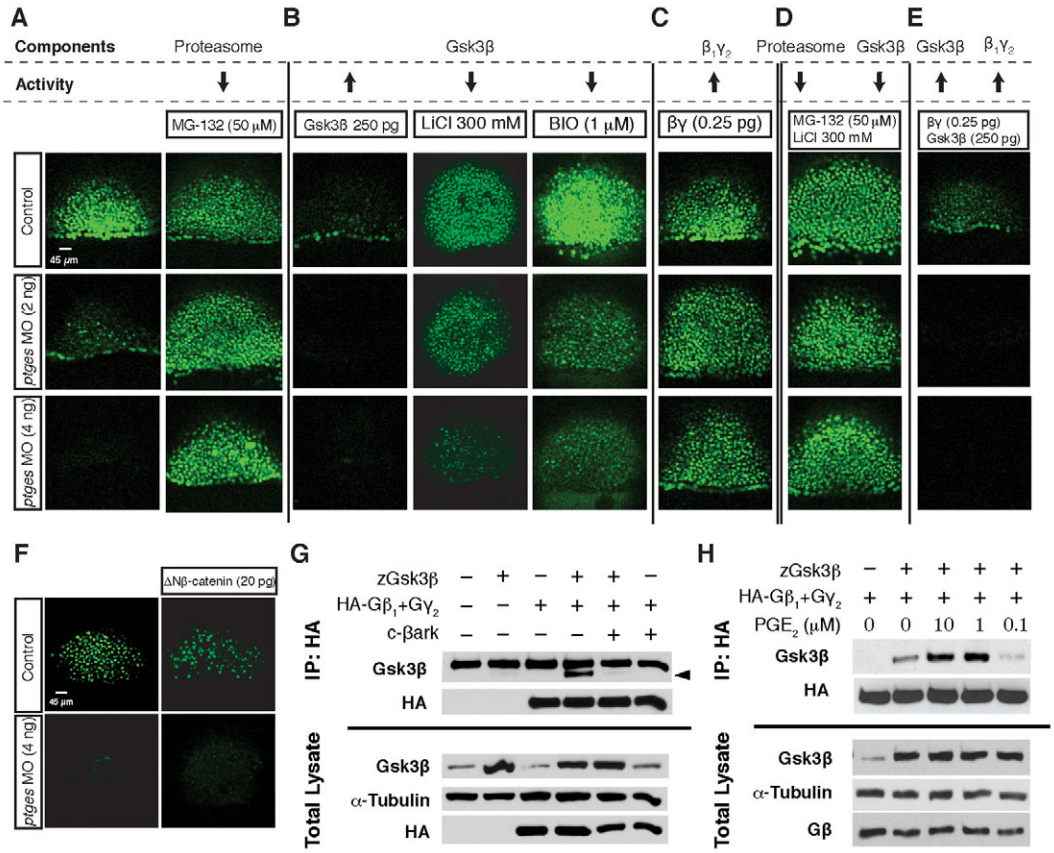

Fig. 5. PGE_2/Gβγ signaling stabilizes Snai1 by inhibiting Gsk3β-mediated proteasomal degradation. (**A-E**) Confocal images of zebrafish embryos in which the Snai1a-YFP assay was used to test downstream components of PGE_2 signaling for their ability to affect levels of Snai1a in control (top row) and *ptges* morphants (middle and bottom rows). (A) Treatment with the proteasome inhibitor MG132. (B) Injection of zebrafish *gsk3*β RNA and treatment with the Gsk3β inhibitors LiCl and BIO. (C) Injection of human $G\beta_1$ and $G\gamma_2$ RNA. (D) Inhibition of both Gsk3β and the proteasome (MG132 treatment). (E) human $G\beta_1\gamma_2$ and zebrafish *gsk3*β RNA co-injection. (**F**) Snai1a-YFP expression in control (top row) and *ptges* morphants (bottom row) injected with RNA encoding constitutively active ΔNβ-catenin. (**G**) Immunoblotting of Gsk3β following immunoprecipitation with human $G\beta_1\gamma_2$. Zebrafish Gsk3β and HA-tagged human $G\beta_1\gamma_2$ were transfected into HEK-293T cells. Cell extracts were immunoprecipitated with anti-HA, then immunoblotted with anti-Gsk3β (Gsk3β indicated by arrowhead). The interaction between Gsk3β and human $G\beta_1\gamma_2$ was blocked by the addition of c-βark (top). Total lysate western blots are shown at the bottom. (**H**) Immunoblotting of Gsk3β following PGE_2 treatment and immunoprecipitation with human $G\beta_1\gamma_2$. Zebrafish Gsk3β and HA-tagged human $G\beta_1\gamma_2$ were transfected into HEK-293T cells, then cells were treated with 0.1, 1 and 10 μM PGE_2 prior to collecting the cell extracts in NDLB. Cell extracts were immunoprecipitated with anti-HA, then immunoblotted with anti-Gsk3β. Total lysate western blots are shown at the bottom.

to enhance β-catenin levels and contribute to hematopoietic stem cell recovery (Goessling et al., 2009). However, we found that the overexpression of ΔNβ-catenin, a constitutively active form, at doses sufficient to induce ectopic body axes in injected embryos (Kelly et al., 1995a) (data not shown) had a minimal effect on Snai1a-YFP expression and could not suppress the decrease in Snai1a-YFP when co-injected with the *ptges* MO (Fig. 5F). Hence, the effect of PGE_2 in stabilizing Snai1a through inhibiting its Gsk3β-mediated degradation does not occur downstream of β-catenin activation.

DISCUSSION

Here, we demonstrate that strong reduction of PGE_2 synthesis by interference with Cox1 and Ptges enzymes impairs all epiboly and internalization gastrulation movements, adding to the previously documented defects in convergence and extension reported at intermediate PGE_2 deficiency (Grosser et al., 2002; Solnica-Krezel, 2005; Cha et al., 2006a). Our data show that these widespread gastrulation defects in PGE_2-deficient embryos are in part due to increased cell-cell adhesion. PGE_2 signaling limits cell adhesion during gastrulation by modulating E-cadherin transcript and protein, in part through stabilization of Snai1. Our results suggest that PGE_2 can regulate the expression of both Snai1a and Snai1b, although Snai1a is much more sensitive to changes in PGE_2 synthesis. *snai1a* and *snai1b* are expressed in different domains of the gastrula (Blanco et al., 2007). Both proteins function non-redundantly in anterior migration of the prechordal plate through repression of E-cadherin. In addition, loss of Snai1b by MO targeting results in a convergence and extension defect. Therefore, it is possible that PGE_2 inhibits E-cadherin via distinct Snai1a- and Snai1b-dependent mechanisms, as Snai1b does not contain complete Gsk3β phosphorylation domains. Determining whether PGE_2 stabilizes Snai1a and Snai1b by distinct mechanisms is an important future direction because each genetic interaction might lead to the regulation of different cell movements. Although their complementary expression patterns suggest that Snai1a and Snai1b

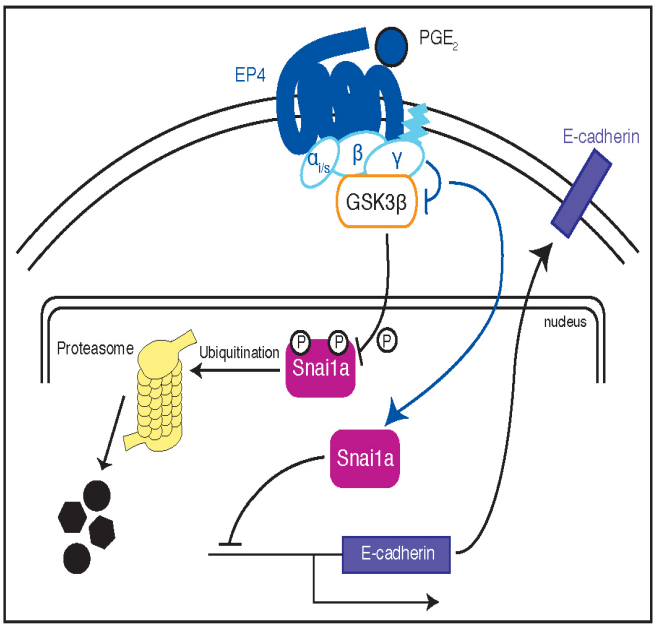

Fig. 6. Model of the mechanism by which zebrafish PGE$_2$ negatively regulates E-cadherin via a Snai1a-dependent mechanism. Following EP4 receptor engagement by PGE$_2$, the Gβγ subunits bind Gsk3β, preventing it from inhibiting Snai1a by phosphorylation. Ubiquitylation of Snail is decreased, stabilizing Snai1a protein. Snai1a can then transcriptionally repress *E-cadherin*, altering the cell adhesion of signaling cells. Blue arrows, pathway mechanism following PGE$_2$ signaling activation.

regulate E-cadherin in different domains of the zebrafish gastrulae, the mosaic overexpression of Snai1a-HA is likely to override this regional specificity. Therefore, we hypothesize that overexpression of either Snai1a-HA or Snai1b-HA in Ptges-deficient embryos would result in the suppression of increased E-cadherin-mediated cell adhesion.

Snai1a-HA overexpression lowered E-cadherin levels in PGE$_2$-deficient gastrulae, but was unable to restore normal gastrulation movements. Similarly, downregulation of E-cadherin by antisense MO suppressed the cell clumping phenotype in the PGE$_2$-deficient gastrulae, but failed to rescue epiboly movements. Because deficiency of E-cadherin alone results in epiboly and other gastrulation defects (Babb and Marrs, 2004; Kane et al., 2005; Shimizu et al., 2005), inhibiting the expression of *cdh1* might not be sufficient to suppress the gastrulation movement phenotype in Ptges-deficient embryos. Another possibility is that unchecked cell adhesion is not the sole contributor to the gastrulation movement defects. Pik3 overexpression was also unable to suppress the gastrulation phenotype of Ptges-deficient embryos, which show defects in Pi3k signaling (Cha et al., 2006a). Therefore, PGE$_2$ may activate Snai1 and Pik3 in parallel to influence gastrulation movements by limiting cell adhesion and enhancing cell motility, respectively. We speculate that PGE$_2$, which is ubiquitously produced during gastrulation (Grosser et al., 2002; Cha et al., 2006a), constantly inhibits E-cadherin expression to ensure the dynamic and precise modulation of E-cadherin levels that is necessary for the massive and dynamic cell movements of gastrulation. In this manner, PGE$_2$ impinges on multiple cellular properties to affect various cell behaviors during gastrulation.

We provide evidence that PGE$_2$ negatively regulates E-cadherin expression in part through the stabilization of Snai1a by preventing its Gsk3β-mediated proteasomal degradation (Fig. 6). PGE$_2$ signaling inhibits Gsk3β via its downstream G protein βγ subunits, a novel molecular mechanism by which PGE$_2$ can promote Snai1a function and limit cell adhesion to influence motility. We have shown that the inhibition of Gsk3β by Gβγ is not dependent on Pik3. Moreover, Gsk3β and Gβγ proteins can be co-immunoprecipitated when expressed in mammalian tissue culture (Fig. 5F,G). Therefore, we present an alternative pathway by which PGE$_2$ can regulate Gsk3β without the need for second messengers. This interaction between Gsk3β and Gβγ proteins has also been observed in human cell culture [Gβγ promotes LRP6-mediated β-catenin/TCF signaling by stimulating plasma membrane localization and activation of GSK3 (K.K.J., C. S. Cselenyi, C. Thorne, N. Hajicek, W. Oldham, L. A. Lee, H. E. Hamm, J. R. Hepler, T. Kozasa, M. E. Linder and E.L., unpublished)], suggesting that this mechanism occurs in multiple cellular contexts and vertebrate species. Although the molecular mechanism by which Gβγ inhibits Gsk3β during gastrulation remains to be elucidated, the work by Jernigan et al. suggests that Gβγ binds GSK3β, sequestering it to the membrane to activate its kinase activity on the co-receptor LRP6, leading to the inhibition of β-catenin degradation and the potentiation of β-catenin/TCF-mediated transcription. In addition, in breast cancer cells, the presence of GSK3β in the nucleus is essential for its silencing of SNAI1 activity. When AXIN2 acts as a nucleocytoplasmic chaperone for GSK3β, exporting it from the nucleus, SNAI1 remains active (Yook et al., 2006). Therefore, we speculate that following activation by PGE$_2$, Gβγ binds Gsk3β at the membrane to prevent it from inhibiting Snai1a activity in the nucleus.

Although our data suggest that PGE$_2$ does not regulate Snai1a stability via β-catenin, it is still possible that PGE$_2$ activates β-catenin by the inhibition of Gsk3β. Interestingly, a previous study has shown that β-catenin can repress *Cdh1* transcription through noggin-activated LEF1 in mouse hair follicles (Jamora et al., 2003). If this mechanism also operates in gastrulae, PGE$_2$ might employ β-catenin-dependent and -independent mechanisms to repress *cdh1* expression. However, as we have previously demonstrated, PGE$_2$-deficient gastrulae show relatively normal axis specification (Cha et al., 2006a), suggesting that PGE$_2$ and Wnt/β-catenin might interact differently depending on the cellular context.

Snai1 expression is increased in multiple tumor types (Barrallo-Gimeno and Nieto, 2005; Yook et al., 2006) and promotes the recurrence of breast cancer in vivo (Moody et al., 2005). In addition, the activation of EGF signaling, which plays a major role in many cancers, increases the expression of Snai1, emphasizing its role during tumorigenesis (Lu et al., 2003; Mann et al., 2006; Backlund et al., 2008). PGE$_2$ signaling has been correlated with increased cancer cell invasiveness, angiogenesis and anchorage independence (Wang and Dubois, 2006), properties that allow cancer cells to exit the primary tumor and migrate to secondary sites (metastasis). Increased expression of the EP4 receptor has also been reported in colon and breast cancer cells (Chell et al., 2006), indicating that cancer cells can utilize native regulation of the cell motility machinery by PGE$_2$. Therefore, our discovery of the Snai1a-dependent repression of cell adhesion by PGE$_2$ might lend insight into the mechanism by which prostaglandins promote tumor cell motility and metastasis. Because Wnt signaling also inhibits Gsk3β activity, Wnt and PGE$_2$ pathways can converge, via β-catenin, to promote hematopoietic stem cell survival (North et al., 2007; Goessling et al., 2009). We suggest that the Wnt and PGE$_2$ pathways

might also promote cell motility by inhibiting cell adhesion. We also speculate that the repression of E-cadherin by PGE_2 might apply to other roles of prostaglandins/PGE_2, for example in inflammation and hematopoietic stem cell recovery.

Acknowledgements
We thank L.S.-K. laboratory members for helpful discussions and comments; Heidi Beck and the SC Facility Research Assistants for fish care; Drs M. Hammerschmidt (Snai1 antibody), J. A. Marrs (zCdh1 antibody), T. Hirano (Snai1a-YFP construct), M. Hibi (zGsk3β construct), A. Nieto (Snai1b construct), C. Wright (zNdr2 construct), and C. Hong and K. Friedman for providing experimental reagents. Confocal experiments were performed in the VUMC Cell Imaging Core Facility (supported by NIH grant 1S10RR015682). This work was supported in part by NIH grant GM77770 to L.S.-K. Deposited in PMC for release after 12 months.

Competing interests statement
The authors declare no competing financial interests.

Supplementary material
Supplementary material for this article is available at
http://dev.biologists.org/lookup/suppl/doi:10.1242/dev.045971/-/DC1

References
Babb, S. G. and Marrs, J. A. (2004). E-cadherin regulates cell movements and tissue formation in early zebrafish embryos. *Dev. Dyn.* **230**, 263-277.
Backlund, M. G., Mann, J. R., Holla, V. R., Shi, Q., Daikoku, T., Dey, S. K. and DuBois, R. N. (2008). Repression of 15-hydroxyprostaglandin dehydrogenase involves histone deacetylase 2 and snail in colorectal cancer. *Cancer Res.* **68**, 9331-9337.
Barrallo-Gimeno, A. and Nieto, M. A. (2005). The Snail genes as inducers of cell movement and survival: implications in development and cancer. *Development* **132**, 3151-3161.
Blanco, M. J., Barrallo-Gimeno, A., Acloque, H., Reyes, A. E., Tada, M., Allende, M. L., Mayor, R. and Nieto, M. A. (2007). Snail1a and Snail1b cooperate in the anterior migration of the axial mesendoderm in the zebrafish embryo. *Development* **134**, 4073-4081.
Blaser, H., Eisenbeiss, S., Neumann, M., Reichman-Fried, M., Thisse, B., Thisse, C. and Raz, E. (2005). Transition from non-motile behaviour to directed migration during early PGC development in zebrafish. *J. Cell Sci.* **118**, 4027-4038.
Brouxhon, S., Kyrkanides, S., O'Banion, M. K., Johnson, R., Pearce, D. A., Centola, G. M., Miller, J. N., McGrath, K. H., Erdle, B., Scott, G., et al. (2007). Sequential down-regulation of E-cadherin with squamous cell carcinoma progression: loss of E-cadherin via a prostaglandin E2-EP2 dependent posttranslational mechanism. *Cancer Res.* **67**, 7654-7664.
Buchanan, F. G. and Dubois, R. N. (2006). Connecting COX-2 and Wnt in cancer. *Cancer Cell* **9**, 6-8.
Carver, E. A., Jiang, R., Lan, Y., Oram, K. F. and Gridley, T. (2001). The mouse snail gene encodes a key regulator of the epithelial-mesenchymal transition. *Mol. Cell. Biol.* **21**, 8184-8188.
Castellone, M. D., Teramoto, H., Williams, B. O., Druey, K. M. and Gutkind, J. S. (2005). Prostaglandin E2 promotes colon cancer cell growth through a Gs-axin-beta-catenin signaling axis. *Science* **310**, 1504-1510.
Cha, Y. I., Kim, S. H., Sepich, D., Buchanan, F. G., Solnica-Krezel, L. and Dubois, R. N. (2006a). Cyclooxygenase-1-derived PGE2 promotes cell motility via the G-protein-coupled EP4 receptor during vertebrate gastrulation. *Genes Dev.* **20**, 77-86.
Cha, Y. I., Solnica-Krezel, L. and Dubois, R. N. (2006b). Fishing for prostanoids: Deciphering the developmental functions of cyclooxygenase-derived prostaglandins. *Dev. Biol.* **289**, 263-272.
Chell, S. D., Witherden, I. R., Dobson, R. R., Moorghen, M., Herman, A. A., Qualtrough, D., Williams, A. C. and Paraskeva, C. (2006). Increased EP4 receptor expression in colorectal cancer progression promotes cell growth and anchorage independence. *Cancer Res.* **66**, 3106-3113.
Dohadwala, M., Yang, S. C., Luo, J., Sharma, S., Batra, R. K., Huang, M., Lin, Y., Goodglick, L., Krysan, K., Fishbein, M. C., et al. (2006). Cyclooxygenase-2-dependent regulation of E-cadherin: prostaglandin E(2) induces transcriptional repressors ZEB1 and snail in non-small cell lung cancer. *Cancer Res.* **66**, 5338-5345.
Doitsidou, M., Reichman-Fried, M., Stebler, J., Koprunner, M., Dorries, J., Meyer, D., Esguerra, C. V., Leung, T. and Raz, E. (2002). Guidance of primordial germ cell migration by the chemokine SDF-1. *Cell* **111**, 647-659.
Dominguez, D., Montserrat-Sentis, B., Virgos-Soler, A., Guaita, S., Grueso, J., Porta, M., Puig, I., Baulida, J., Franci, C. and Garcia de Herreros, A. (2003). Phosphorylation regulates the subcellular location and activity of the snail transcriptional repressor. *Mol. Cell. Biol.* **23**, 5078-5089.
Drees, F., Pokutta, S., Yamada, S., Nelson, W. J. and Weis, W. I. (2005). Alpha-catenin is a molecular switch that binds E-cadherin-beta-catenin and regulates actin-filament assembly. *Cell* **123**, 903-915.
Erter, C. E., Solnica-Krezel, L. and Wright, C. V. (1998). Zebrafish nodal-related 2 encodes an early mesendodermal inducer signaling from the extraembryonic yolk syncytial layer. *Dev. Biol.* **204**, 361-372.
Fujino, H. and Regan, J. W. (2003). Prostanoid receptors and phosphatidylinositol 3-kinase: a pathway to cancer? *Trends Pharmacol. Sci.* **24**, 335-340.
Fujino, H., West, K. A. and Regan, J. W. (2002). Phosphorylation of glycogen synthase kinase-3 and stimulation of T-cell factor signaling following activation of EP2 and EP4 prostanoid receptors by prostaglandin E2. *J. Biol. Chem.* **277**, 2614-2619.
Goessling, W., North, T. E., Loewer, S., Lord, A. M., Lee, S., Stoick-Cooper, C. L., Weidinger, G., Puder, M., Daley, G. Q., Moon, R. T. et al. (2009). Genetic interaction of PGE2 and Wnt signaling regulates developmental specification of stem cells and regeneration. *Cell* **136**, 1136-1147.
Gritsman, K., Zhang, J., Cheng, S., Heckscher, E., Talbot, W. S. and Schier, A. F. (1999). The EGF-CFC protein one-eyed pinhead is essential for nodal signaling. *Cell* **97**, 121-132.
Grosser, T., Yusuff, S., Cheskis, E., Pack, M. A. and FitzGerald, G. A. (2002). Developmental expression of functional cyclooxygenases in zebrafish. *Proc. Natl. Acad. Sci. USA* **99**, 8418-8423.
Hammerschmidt, M. and Nusslein-Volhard, C. (1993). The expression of a zebrafish gene homologous to Drosophila snail suggests a conserved function in invertebrate and vertebrate gastrulation. *Development* **119**, 1107-1118.
Hammerschmidt, M. and Wedlich, D. (2008). Regulated adhesion as a driving force of gastrulation movements. *Development* **135**, 3625-3641.
Jamora, C., DasGupta, R., Kocieniewski, P. and Fuchs, E. (2003). Links between signal transduction, transcription and adhesion in epithelial bud development. *Nature* **422**, 317-322.
Kane, D. A., McFarland, K. N. and Warga, R. M. (2005). Mutations in half baked/E-cadherin block cell behaviors that are necessary for teleost epiboly. *Development* **132**, 1105-1116.
Kelly, G. M., Erezyilmaz, D. F. and Moon, R. T. (1995a). Induction of a secondary embryonic axis in zebrafish occurs following the overexpression of beta-catenin. *Mech. Dev.* **53**, 261-273.
Kelly, G. M., Greenstein, P., Erezyilmaz, D. F. and Moon, R. T. (1995b). Zebrafish wnt8 and wnt8b share a common activity but are involved in distinct developmental pathways. *Development* **121**, 1787-1799.
Kim, S. H., Park, H. C., Yeo, S. Y., Hong, S. K., Choi, J. W., Kim, C. H., Weinstein, B. M. and Huh, T. L. (1998). Characterization of two frizzled8 homologues expressed in the embryonic shield and prechordal plate of zebrafish embryos. *Mech. Dev.* **78**, 193-201.
Kimmel, C. B., Ballard, W. W., Kimmel, S. R., Ullmann, B. and Schilling, T. F. (1995). Stages of embryonic development of the zebrafish. *Dev. Dyn.* **203**, 253-310.
Leopoldt, D., Hanck, T., Exner, T., Maier, U., Wetzker, R. and Nurnberg, B. (1998). Gbetagamma stimulates phosphoinositide 3-kinase-gamma by direct interaction with two domains of the catalytic p110 subunit. *J. Biol. Chem.* **273**, 7024-7029.
Lin, F., Sepich, D. S., Chen, S., Topczewski, J., Yin, C., Solnica-Krezel, L. and Hamm, H. (2005). Essential roles of G{alpha}12/13 signaling in distinct cell behaviors driving zebrafish convergence and extension gastrulation movements. *J. Cell Biol.* **169**, 777-787.
Lin, F., Chen, S., Sepich, D. S., Panizzi, J. R., Clendenon, S. G., Marrs, J. A., Hamm, H. E. and Solnica-Krezel, L. (2009). Galpha12/13 regulate epiboly by inhibiting E-cadherin activity and modulating the actin cytoskeleton. *J. Cell Biol.* **184**, 909-921.
Lu, Z., Ghosh, S., Wang, Z. and Hunter, T. (2003). Downregulation of caveolin-1 function by EGF leads to the loss of E-cadherin, increased transcriptional activity of beta-catenin, and enhanced tumor cell invasion. *Cancer Cell* **4**, 499-515.
Mann, J. R., Backlund, M. G., Buchanan, F. G., Daikoku, T., Holla, V. R., Rosenberg, D. W., Dey, S. K. and DuBois, R. N. (2006). Repression of prostaglandin dehydrogenase by epidermal growth factor and snail increases prostaglandin E2 and promotes cancer progression. *Cancer Res.* **66**, 6649-6656.
McFarland, K. N., Warga, R. M. and Kane, D. A. (2005). Genetic locus half baked is necessary for morphogenesis of the ectoderm. *Dev. Dyn.* **233**, 390-406.
Montero, J. A. and Heisenberg, C. P. (2004). Gastrulation dynamics: cells move into focus. *Trends Cell Biol.* **14**, 620-627.
Montero, J. A., Kilian, B., Chan, J., Bayliss, P. E. and Heisenberg, C. P. (2003). Phosphoinositide 3-kinase is required for process outgrowth and cell polarization of gastrulating mesendodermal cells. *Curr. Biol.* **13**, 1279-1289.
Montero, J. A., Carvalho, L., Wilsch-Brauninger, M., Kilian, B., Mustafa, C. and Heisenberg, C. P. (2005). Shield formation at the onset of zebrafish gastrulation. *Development* **132**, 1187-1198.
Moody, S. E., Perez, D., Pan, T. C., Sarkisian, C. J., Portocarrero, C. P., Sterner, C. J., Notorfrancesco, K. L., Cardiff, R. D. and Chodosh, L. A. (2005). The transcriptional repressor Snail promotes mammary tumor recurrence. *Cancer Cell* **8**, 197-209.

North, T. E., Goessling, W., Walkley, C. R., Lengerke, C., Kopani, K. R., Lord, A. M., Weber, G. J., Bowman, T. V., Jang, I. H., Grosser, T., et al. (2007). Prostaglandin E2 regulates vertebrate haematopoietic stem cell homeostasis. *Nature* **447**, 1007-1011.
Pacquelet, A. and Rorth, P. (2005). Regulatory mechanisms required for DE-cadherin function in cell migration and other types of adhesion. *J. Cell Biol.* **170**, 803-812.
Regan, J. W. (2003). EP2 and EP4 prostanoid receptor signaling. *Life Sci.* **74**, 143-153.
Schulte-Merker, S., Ho, R. K., Herrmann, B. G. and Nusslein-Volhard, C. (1992). The protein product of the zebrafish homologue of the mouse T gene is expressed in nuclei of the germ ring and the notochord of the early embryo. *Development* **116**, 1021-1032.
Shimizu, T., Yabe, T., Muraoka, O., Yonemura, S., Aramaki, S., Hatta, K., Bae, Y. K., Nojima, H. and Hibi, M. (2005). E-cadherin is required for gastrulation cell movements in zebrafish. *Mech. Dev.* **122**, 747-763.
Solnica-Krezel, L. (2005). Conserved patterns of cell movements during vertebrate gastrulation. *Curr. Biol.* **15**, R213-R228.
Solnica-Krezel, L. (2006). Gastrulation in zebrafish – all just about adhesion? *Curr. Opin. Genet. Dev.* **16**, 433-441.
Stachel, S. E., Grunwald, D. J. and Myers, P. Z. (1993). Lithium perturbation and goosecoid expression identify a dorsal specification pathway in the pregastrula zebrafish. *Development* **117**, 1261-1274.
Thisse, B. and Thisse, C. (1998). High resolution whole-mount in situ hybridization. *Zebrafish Science Monitor* **5**, 8-9.
Tingaud-Sequeira, A., Andre, M., Forgue, J., Barthe, C. and Babin, P. J. (2004). Expression patterns of three estrogen receptor genes during zebrafish (Danio rerio) development: evidence for high expression in neuromasts. *Gene Expr. Patterns* **4**, 561-568.
Ulrich, F., Krieg, M., Schotz, E. M., Link, V., Castanon, I., Schnabel, V., Taubenberger, A., Mueller, D., Puech, P. H. and Heisenberg, C. P. (2005). Wnt11 functions in gastrulation by controlling cell cohesion through Rab5c and E-cadherin. *Dev. Cell* **9**, 555-564.
von der Hardt, S., Bakkers, J., Inbal, A., Carvalho, L., Solnica-Krezel, L., Heisenberg, C. P. and Hammerschmidt, M. (2007). The Bmp gradient of the zebrafish gastrula guides migrating lateral cells by regulating cell-cell adhesion. *Curr. Biol.* **17**, 475-487.
Wang, D. and Dubois, R. N. (2006). Prostaglandins and cancer. *Gut* **55**, 115-122.
Wu, S. Y. and McClay, D. R. (2007). The Snail repressor is required for PMC ingression in the sea urchin embryo. *Development* **134**, 1061-1070.
Wu, T. (2006). Cyclooxygenase-2 in hepatocellular carcinoma. *Cancer Treat. Rev.* **32**, 28-44.
Yamashita, S., Miyagi, C., Fukada, T., Kagara, N., Che, Y. S. and Hirano, T. (2004). Zinc transporter LIVI controls epithelial-mesenchymal transition in zebrafish gastrula organizer. *Nature* **429**, 298-302.
Yook, J. I., Li, X. Y., Ota, I., Hu, C., Kim, H. S., Kim, N. H., Cha, S. Y., Ryu, J. K., Choi, Y. J., Kim, J., et al. (2006). A Wnt-Axin2-GSK3beta cascade regulates Snail1 activity in breast cancer cells. *Nat. Cell Biol.* **8**, 1398-1406.
Zhou, B. P., Deng, J., Xia, W., Xu, J., Li, Y. M., Gunduz, M. and Hung, M. C. (2004). Dual regulation of Snail by GSK-3beta-mediated phosphorylation in control of epithelial-mesenchymal transition. *Nat. Cell Biol.* **6**, 931-940.
Zohn, I. E., Li, Y., Skolnik, E. Y., Anderson, K. V., Han, J. and Niswander, L. (2006). p38 and a p38-interacting protein are critical for downregulation of E-cadherin during mouse gastrulation. *Cell* **125**, 957-969.